Contactless sleep posture measurements for demand-controlled sleep thermal comfort: A pilot study

Article *in* Indoor Air · December 2022

DOI: 10.1111/ina.13175

5 authors, including:

Xiaogang Cheng
Nanjing University of Posts and Telecommunications
33 PUBLICATIONS **552** CITATIONS
SEE PROFILE

Bin Yang
Tianjin Chengjian University
300 PUBLICATIONS **3,565** CITATIONS
SEE PROFILE

Faming Wang
KUL/PolyU/XUST
325 PUBLICATIONS **5,249** CITATIONS
SEE PROFILE

Thomas Olofsson
Umeå University
157 PUBLICATIONS **2,788** CITATIONS
SEE PROFILE

Received: 25 August 2022 | Revised: 18 October 2022 | Accepted: 24 October 2022

DOI: 10.1111/ina.13175

ORIGINAL ARTICLE

WILEY

Contactless sleep posture measurements for demand-controlled sleep thermal comfort: A pilot study

Xiaogang Cheng[1,2] | Fei Hu[1] | Bin Yang[2,3] | Faming Wang[4] | Thomas Olofsson[2]

[1]College of Telecommunications and Information Engineering, Nanjing University of Posts and Telecommunications, Nanjing, China

[2]Department of Applied Physics and Electronics, Umeå University, Umeå, Sweden

[3]School of Energy and Safety Engineering, Tianjing Chengjian University, Tianjin, China

[4]Department of Biosystems (BIOSYST), KU Leuven, Leuven, Belgium

Correspondence
Bin Yang, School of Energy and Safety Engineeing, Tianjin Chengjian University, Tianjin, China.
Email: binyang@tcu.edu.cn

Funding information
Social Development Project of Jiangsu Key R&D Program, Grant/Award Number: BE2022680; National Natural Science Foundation of China, Grant/Award Number: 61972214 and 52278119; Ministry of Industry and Information Technology of China, Grant/Award Number: 2021-R-43; Jiangsu Postdoctoral Science Foundation, Grant/Award Number: 1601039B

Abstract

Thermal comfort during sleep is essential for both sleep quality and human health while sleeping. There are currently few effective contactless methods for detecting the sleep thermal comfort at any time of day or night. In this paper, a vision-based detection approach for human thermal comfort while sleeping was proposed, which is intended to avoid overcooling/overheating supply, meet the thermal comfort needs of human sleep, and improve human sleep quality and health. Based on 438 valid questionnaire surveys, 10 types of thermal comfort sleep postures were summarized. By using a large number of data captured, a fundamental framework of detection algorithm was constructed to detect human sleeping postures, and corresponding weighting model was established. A total of 2.65 million frames of posture data in natural sleep status were collected, and thermal comfort-related sleep postures dataset was created. Finally, the robustness and effectiveness of the proposed algorithm were validated. The validation results show that the sleeping posture and human skeleton keypoints can be used for estimating sleeping thermal comfort, and the the quilt coverage area can be fused to improve the detection accuracy.

KEYWORDS
contactless measurements, deep learning, pose estimation, sleep posture, sleep quality, sleep thermal comfort

1 | INTRODUCTION

Sleep quality is essential to human health. According to World Health Organization data, 27% of people worldwide have sleep problems, 38.2% of Chinese adults have insomnia, and more than 300 million Chinese have sleep disorders.[2] Currently, the commonly used methods of sleep quality detection are contact-based methods; however, this kind of method can exacerbate personal sleep disorders.[3,4] Therefore, there is an urgent need to study effective contactless detection methods.

Nowadays, there are two types of sleep state detection methods: contact-detection methods[5–13] and contactless detection methods.[14–25] The contactless method is further classified into two types: (1) audio-based method[14–17] and (2) vision-based method.[18–25] In terms of the contact-detection method, some wearable devices were used to human body and collect personal information about sleep state.[5–13] The contact method of sleep state detection necessitates the use of wearable equipment, which affects people's sleep states and causes "first night effect" lasting for several days. True sleep state, without disturbances from wearable devices, is almost impossible to be achieved. Kripke et al.[10] stated that the algorithm of detecting sleep or awake state from activity record data is less sensitive because the detection rate of awake state is low. Machine learning was adopted to analyze wrist activity information of sleep.[12,13]

Because of the shortcomings of contact methods, contactless detection method has been studied and is becoming popular.

In terms of the audio-based contactless method, language detection and video detection are the two broad categories. The audio-based method requires human subject to snore loudly during sleep.[14–17] Meanwhile, surrounding environments remain quiet. Dafna et al.[14,15] proposed a new sleep quality analysis system based on sound signal processing and audio signal examination. Wu et al[16] used the hierarchical clustering and self-organization graph of Kullback–Leibler kernel to classify the data as good or bad sleep. Maximum accuracy (70%) was achieved using five hidden states. Xue et al[17] investigated a sleep stage detection method with breathing sounds. The time-domain and frequency-domain features of breathing sounds were extracted. This method outperforms current methods and is expected to be used in large-scale contactless sleep monitoring. Because of strict requirements for the audio-based method, the vision-based method is gaining popularity for detecting sleep state. Peng et al[18] developed a multimodal sensor system with multisensors. The signals were classified using support vector machine, and the output was fused together to infer sleep quality. Choe et al[19] used machine learning to develop an automatic VSG method for establishing a relationship model between human head movement and sleep state. Cheng et al[20] used a deep convolutional network to construct a relationship between human skin texture features and subtle movements and human body temperature, thereby human thermal comfort could be obtained. Further, Cheng et al[21,22] established the link between skin variation and human thermal comfort. Meier et al[23] found that when people are thermally uncomfortable, they adopt unique poses or actions. When a discomfort-related gesture is detected, it is scored based on the gesture type and recognition confidence. Cheng et al[24] proposed a new method based on contactless measurement of human thermal discomfort. The red green blue (RGB) camera captures an image of the occupant's posture related to the body temperature. An algorithm was developed to recognize different postures related to thermal discomfort. Cheng et al[25] used Openpose to obtain the human body posture information and constructed an algorithm to detect five types of real-time thermal discomfort motions. Based on sensor of infrared thermal imaging, Li[26,27] collected human face data and constructed a comprehensive system framework to predict human age and gender and thermal comfort. The difference between RGB image and infrared thermal images was discussed in predicting age and gender, and the impact of building usage on human thermal comfort was also assessed.

The aforementioned research indicates that the vision-based method aids in capturing more sleep-related data, while human posture is useful for analyzing thermal comfort. In the meantime, human posture recognition has advanced significantly in recent years, both for single and multiple individuals. In terms of pose recognition of single person, Chen et al[28,29] proposed pose recognition methods and a structure perception network. Toshev et al[30] proposed a deep neural network (DNN)-based human posture estimation method, which was the first application of DNNs in human posture estimation. Pfister et al[31] proposed a Flowing ConvNets network that treated attitude estimation as a detection problem and outputted a heatmap. But postural predictions that are biologically implausible can be made in this case. To address this issue, Chen et al[32] proposed a new type of structure-sensing convolutional network that implicitly considered prior knowledge in the deep network training process to improve the final pose recognition. In terms of pose recognition of multiperson, Pishchulin et al[33] proposed the DeepCut algorithm in the field of multiperson pose recognition, which is the first work in the field. In the same year, Insafutdinov et al[34] proposed DeeperCut as an improvement on DeepCut. Cao et al[35] proposed the OpenPose algorithm which advances the development of multiperson pose recognition. Guler et al[36] proposed a dense human body pose estimation algorithm. Li et al[37] proposed a new and effective method to solve the crowd pose estimation problem. In recent years, more pose estimation methods have been proposed which are a significant source of inspiration for estimating thermal comfort during sleep.[38–46] Therefore, Mohammadi et al[47] studied sleep pose detection with camera, and Piriyajitakonkij et al[48] studied sleep status with ultra-wideband. All of these are aimed at improving the accuracy of pose estimation in a crowded outdoor crowd, but they do not significantly improve sleep pose detection but instead increase computational complexity.

To overcome the limitations of current methods, it is urgent to study a kind of detection technology of sleep state with the following functions, they are (1) human sleep states are not affected, (2) physiological parameters about human health are collected in real time, and (3) contactless detection method with human-centered logos. Therefore, an end-to-end contactless method for detecting human thermal comfort during sleep was proposed in this paper. The algorithm framework was built using the residual

Practical Implications

The study proposes an alternate approach for controlling the air conditioner in a bedroom by sensing sleep positions in real time using computer vision technologies. Traditional remote controls may overestimate thermal requirements by prolonging cooling in an inefficient manner or underestimate thermal requirements by terminating cooling prematurely. Using the remote control again after a sleep-inducing delay may impair sleep quality. The aforementioned problem can be solved by monitoring sleep postures in real time using computer vision technologies. During the late night and early morning, an increase in air temperature and a decrease in air velocity can better fulfill the needs of sleeping persons, thereby improving sleep quality.[1] Privacy can be safeguarded simply by using sensing data to control rather than recording data.

idea and long short-term memory, which was validated by a large number of data collected. The main contributions of this study are given as follows:

1. A total of 438 questionnaire surveys were collected, from which 10 sleeping postures related to thermal comfort were defined.
2. Under natural sleep state of human subjects, large amounts of data on sleep postures (2.65 million frames) were collected to create a thermal comfort sleep posture dataset (SPC).
3. A fundamental algorithm framework for detecting sleep postures and quilt covered area was built, which was validated by large number of data captured.

2 | METHODS

To achieve the best thermal comfort of human body, an algorithm framework shown in Figure 1 was built. With a normal RGB camera, sleeping video of human subjects during their natural sleep state was captured, as well as quilt covered area. Finally, the thermal comfort of human body was obtained by combining the two aspects above, which are sleep state and quilt covered area.

2.1 | Sleep posture dataset

In this paper, a large number of data was collected and a dataset of human thermal comfort sleep postures (SPC) was constructed. To collect data, some normal RGB cameras were used. The camera's corresponding pixels are 1.3 million, and the video frame rate is 25 frames per second (fps). The camera was fixed beside the bed in a normal sleep room, and the human subject was within the camera's field of view. A total of 2.65 million images of sleeping posture were collected from 18 male subjects for the study. All sleeping trials were carried out in a climate chamber at temperatures ranging from 28 to 35°C during the summer months of July and August. The subjects slept in short pants, and the clothing insulation is 0.20 *clo*.

A questionnaire survey of sleeping posture was conducted, and a total of 438 valid questionnaires were collected. These postures are primarily classified based on 3 factors: (1) the body posture feature, such as curling or stretched, (2) the extent to which the body is covered by the quilt, such as covering below the neck, covering the abdomen and below, and covering the abdomen solely, (3) whether the arms are inside or outside the quilt. Table 1 shows the characteristics of the 10 major sleep postures and their accompanying thermal comfort state, which was classified into three levels: comfortable, cold, and warm. In order to facilitate the practical implementation of the algorithm proposed, three thermal comfort levels intead of seven thermal comfort levels were adopted in this paper. The 10 sleeping postures and their corresponding thermal comfort levels were obtained through questionnaires.

The questionnaire's respondents fall into three categories: (1) fear of cold, (2) fear of heat, and (3) no particular preference. The respondents' ages are dispersed across all age groups above the age of 18. In terms of height, some repondents are taller than 190 cm, while others are shorter than 160 cm, and the majority are between 160 and 190 cm. In terms of weight, some repondents weigh more than 80 kg, while others weigh less than 40 kg, and the majority falling somewhere between 40 and 80 kg.

A total of 18 male subjects (age: 23.9 ± 3.1; height: 1.76 ± 0.09 m; weight: 70.9 ± 30.1 kg; body mass index: 23.0 ± 6.5 kg/m^2) were invited to lie on a bed equipped with a standard camera. To avoid interfering with the experiment, the human subjects were asked to remove their upper body clothing. Then, a large number of sleep posture data (2.65 million images) were collected.

2.2 | Sleep posture recognition of thermal comfort

2.2.1 | Capture skeleton keypoints of human body

Keypoint information of human body was obtained using skeleton keypoint estimation networks. The coordinates of keypoints were used to construct the posture recognition model of human body, and sleep postures were classified as stretched or curled up. Based on the video stream data, the estimation algorithm of keypoints could be used to estimate the keypoint information of the human body. Then, the human pose estimation algorithm was created to estimate the sleep-related posture and evaluate the human thermal comfort while sleeping. The skeleton keypoints of human body required in this paper are shown in Table 2. The algorithm framework, including model I and model II, is shown in Figure 1.

Based on the features of sleep postures, six keypoints of legs (points 9–14) and six keypoints (points 2–7) of arms were focused, which are (1) *legs related*: 9: right hip, 10: right knee, 11: right ankle, 12: left hip, 13: left knee, 14: left ankle; (2) *arms related*: 2: right shoulder, 3: right elbow, 4: right wrist, 5: left shoulder, 6: left elbow, 7: left wrist. In general, two class sleep postures characterized by curling and stretching were defined in this paper. The angle between leg and arm, the displacement of the keypoints, the Euclidean distance between the keypoints, and the cross-validation were adopted to estimate the sleep postures of human body.

The estimation of human skeleton points is an important prerequisite for sleep posture estimation. The input of captured model is the sleep images collected, and the corresponding output is the structured information of skeleton keypoints. If the skeleton keypoints were captured correctly, the method used to capture them would have no effect on the specific detection results of sleep postures. The current existing methods or innovative deep learning network can be adopted to implement the keypoint estimation. In this paper, the OpenPose was used for obtaining the skeleton keypoints. The captured results are shown in Figure 2.

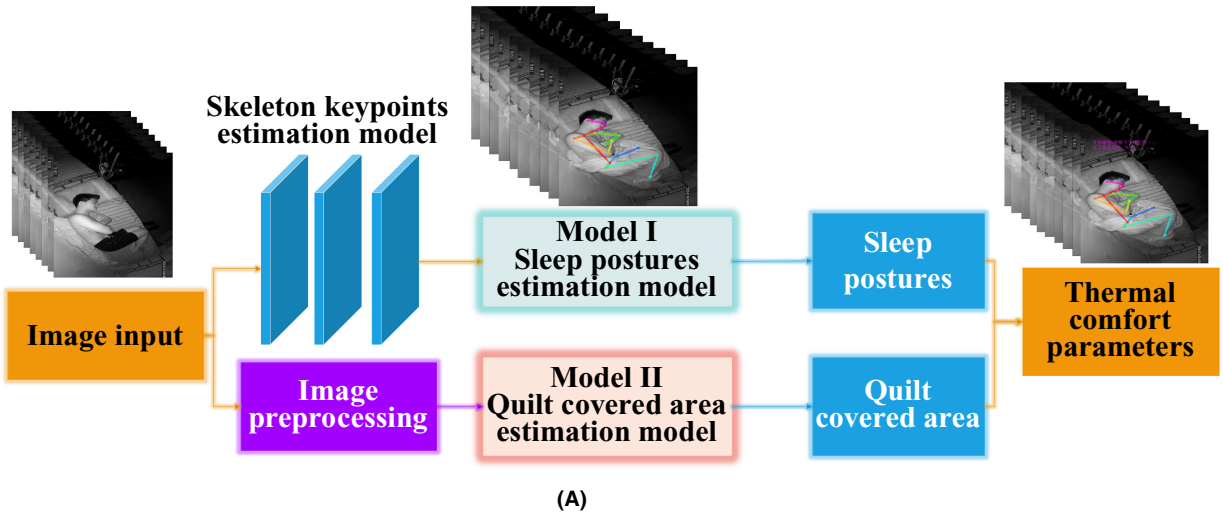

(A)

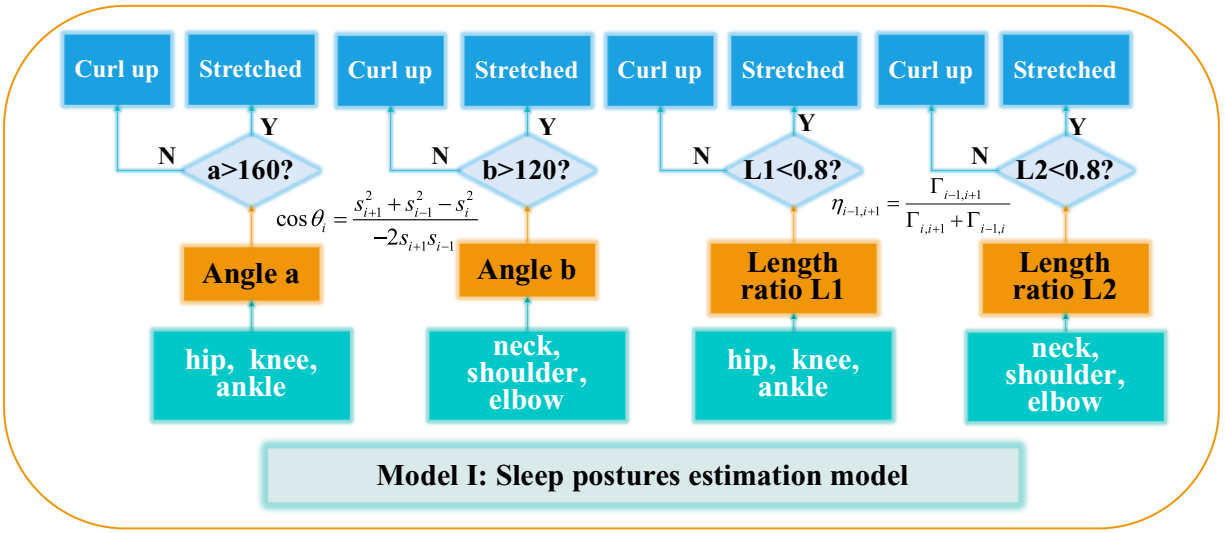

(B)

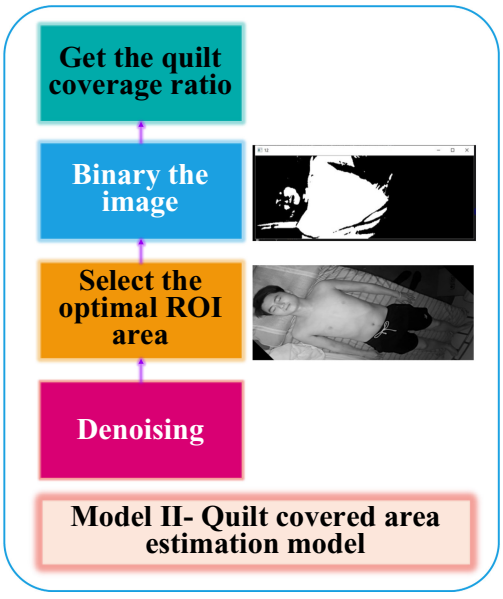

(C)

FIGURE 1 Algorithm framework of sleep posture estimation for thermal comfort (subfigure A is the framework, subfigure B is the details of model I, and subfigure C is the details of model II).

TABLE 1 Sleep posture of human thermal comfort (defined by 438 valid questionnaires).

No.	Sleep postures and quilt coverage	Thermal comfort level
1	Body is stretched, the body parts below neck are covered with quilt, and the arms are covered beneath the quilt	Comfortable
2	Body is stretched, the whole parts below neck are covered with quilt, but the arms are outside the quilt	Comfortable
3	Body is stretched, the belly and lower parts of the body are covered with quilt	Comfortable
4	Body is stretched, only belly of the body is covered with quilt	Comfortable
5	Body is completely stretched and without quilt covered	Warm
6	Body is curled up and without quilt covered	Cold
7	Body is curled up, the body part below neck is covered with quilt, and the arms are covered beneath the quilt	Cold
8	Body is curled up, the body part below neck is covered with quilt, and the arms are covered outside the quilt	Cold
9	Body is curled up, the belly and lower parts of the body are covered with quilt	Comfortable
10	Body is curled up, only belly of the body is covered with quilt	Comfortable

TABLE 2 Mapping relations between skeleton keypoints and body parts.

No.	Coordinate number of keypoints	Body parts	No.	Coordinate number of keypoints	Body parts
1	0	Nose	14	13	Left knee
2	1	Neck	15	14	Left ankle
3	2	Right shoulder	16	15	Right eye
4	3	Right elbow	17	16	Left eye
5	4	Right wrist	18	17	Right ear
6	5	Left shoulder	19	18	Left ear
7	6	Left elbow	20	19	Left big toe
8	7	Left wrist	21	20	Left little toe
9	8	Hip central	22	21	Left heel
10	9	Right hip	23	22	Right big toe
11	10	Right knee	24	23	Right little toe
12	11	Right ankle	25	24	Right heel
13	12	Left hip			

2.2.2 | Detection model of angle between keypoints

Let $i, i+1, i-1$ denote 3 adjacent human skeleton keypoints, $\theta_i, \theta_{i+1}, \theta_{i-1}$ denote the angle between keypoints, and s_i, s_{i+1}, s_{i-1} represents the side length corresponding to the included angle. One of the included angles, θ_i, is calculated as follows:

$$\cos\theta_i = \frac{s_{i+1}^2 + s_{i-1}^2 - s_i^2}{-2s_{i+1}s_{i-1}} \tag{1}$$

In this paper, the skeleton keypoints 1–14 are critical to estimate the stretch or curled angel of the human body. Suppose to calculate the bending degree of human right knee ($\theta_i, i = 10$), the keypoints involved are 9, 10, and 11. Then, s_{i+1} is the length between right hip and right knee, s_{i-1} is the length between right knee and right ankle, and s_i is the length between right hip and right ankle. Suppose to caculate the bending degree of human left knee ($\theta_i, i = 13$), the keypoints related are 12, 13, and 14. Therefore, both θ_{10} and θ_{13} can be obtained by Equation (1). Similarly, if the bending degree of human right elbow ($\theta_i, i = 3$) is estimated, s_{i-1} is the length between keypoint 2 and keypoint 3, s_{i+1} is the length between keypoint 3 and keypoint 4, and s_i is the length between keypoint 2 and 4. If the bending degree of human left elbow ($\theta_i, i = 6$) is caculated, the keypoints involved are left shoulder (keypoint 5), left elbow (keypoint 6), and left wrist (keypoint 7). In practical applications, the elbow or the leg can be selected according to the specific situation, and the degree of stretching and curling of the human body can be recognized, that is, the sleep posture of the human body can be determined by Equation (2).

$$\gamma = \begin{cases} 0 & \min\{\theta_{10}, \theta_{13}\} > \tau_1 \\ 1 & \min\{\theta_{10}, \theta_{13}\} \le \tau_1 \\ 0 & \theta_{10}, \theta_{13} \text{ are not exist} \& \min\{\theta_{10}, \theta_{13}\} \le \upsilon_1 \\ 1 & \theta_{10}, \theta_{13} \text{ are not exist} \& \min\{\theta_{10}, \theta_{13}\} \le \upsilon_1 \end{cases} \tag{2}$$

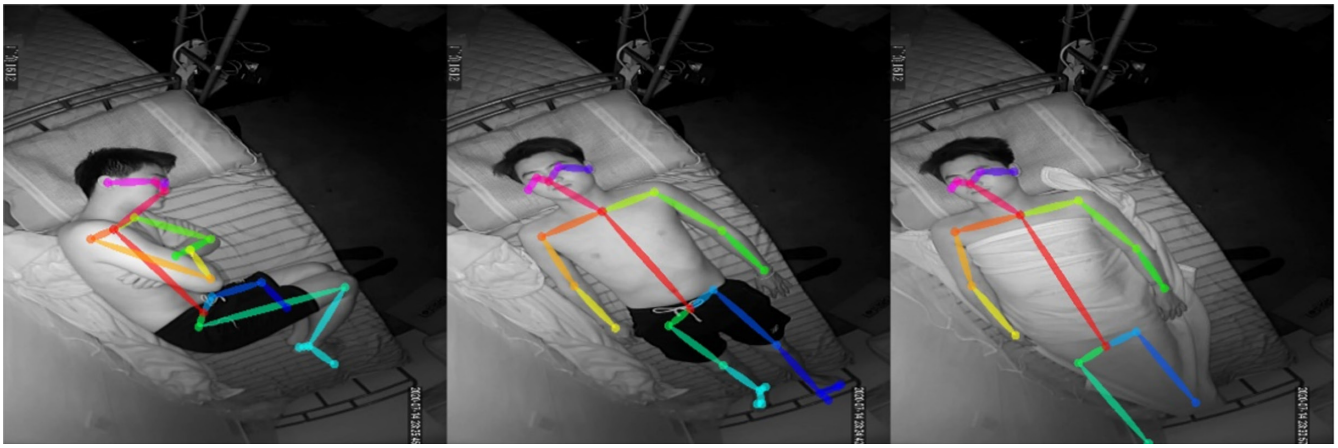

FIGURE 2 Caputured results of human skeleton keypoints.

where γ represents the slee posture class, $\gamma = 0$ represents the stretching posture, and $\gamma = 1$ denotes the crouching posture. θ_{10} is the angle with the right knee as the vertex, and the three keypoints are right knee, right hip, and right ankle. θ_{13} is the angle with the left knee as the vertex, and the corresponding keypoints are left knee, left hip, and left ankle. θ_3 represents the angle with the right elbow as the vertex among the three keypoints of right elbow, right shoulder, and right wrist. θ_6 represents the angle with the left elbow as the vertex among the three keypoints of left elbow, left shoulder, and left wrist. τ_1 represents the leg curling threshold, and υ_1 represents the arm bending threshold. In this paper, the τ_1 belongs to [155, 165] and $\tau_1 = 160$ is adopted. υ_1 belongs to [115, 125], $\tau_1 = 120$ is adopted.

2.2.3 | Detection model of keypoints distance

In order to improve the robustness of estimation algorithm, the Euclidean distance of skeleton keypoints was adopted in cross-validation, and the corresponding equation is shown as follows:

$$\Gamma_{i,i+1} = \left[\left(\alpha_i - \alpha_{i+1}\right)^2 + \left(\beta_i - \beta_{i+1}\right)^2\right]^{1/2} \tag{3}$$

where $\Gamma_{i,i+1}$ is the Euclidean distance of keypoints i and $i+1$, and α_i, β_i are the horizontal and vertical coordinates of the first keypoint, respectively. $\alpha_{i+1}, \beta_{i+1}$ are the horizontal and vertical coordinates of the second keypoint, respectively.

The keypoints of arm skeleton adopted are 9–14. Equation (3) can be used to estimate the distance between right hip and right ankle, that is, $\Gamma_{9,11}$. The distance between left hip and left ankle, $\Gamma_{12,14}$, also can be caculated by Equation (3). In order to improve the detection accuracy, according to the actual situation, both the Euclidean distances of the keypoints on the legs and that on the arms will be caculated, or only one of them was estimated. The six keypoints of arms are keypoints 2–7, the distance from right shoulder to right wrist is $\Gamma_{2,4}$, and the distance from left shoulder to left wrist is $\Gamma_{5,7}$. The $\Gamma_{10,11}$ and $\Gamma_{9,10}$ can also be calculated by Equation (3), then let

$$\eta_{i-1,i+1} = \frac{\Gamma_{i-1,i+1}}{\Gamma_{i,i+1} + \Gamma_{i-1,i}} \tag{4}$$

where $\eta_{i-1,i+1}$ is the scale factor corresponding to the keypoints $i, i-1, i+1$. Based on Equation (4), then

$$\eta_{9,11} = \frac{\Gamma_{9,11}}{\Gamma_{10,11} + \Gamma_{9,10}} \tag{5}$$

Similarly, $\eta_{12,14}, \eta_{2,4}, \eta_{5,7}$ can also be obtained. Then, the state of the sleep postures can be obtained by Equation (6), that is,

$$\psi = \begin{cases} 0 & \min\left\{\eta_{9,11}, \eta_{12,14}\right\} > \tau_2 \\ 1 & \min\left\{\eta_{9,11}, \eta_{12,14}\right\} \le \tau_2 \\ 0 & \eta_{9,11}, \eta_{9,11} \text{ are not exist\&min}\left\{\eta_{2,4}, \eta_{5,7}\right\} > \upsilon_2 \\ 1 & \eta_{9,11}, \eta_{9,11} \text{ are not exist\&min}\left\{\eta_{2,4}, \eta_{5,7}\right\} \le \upsilon_2 \end{cases} \tag{6}$$

where ψ also represents the slee posture class, $\psi = 0$ represents the stretching posture, and $\psi = 1$ represents the curled posture. $\eta_{9,11}, \eta_{12,14}, \eta_{2,4}, \eta_{5,7}$ are scale factors corresponding to right leg, left leg, right arm, and left arm, respectively. τ_2, υ_2 are curled threshold related to distance. The τ_2 correspond to leg which belong to [0.75, 0.85], and $\tau_2 = 0.8$ is adopted in this paper. The υ_2 correspond to arms which also belong to [0.75, 0.85], and $\upsilon_2 = 0.8$ is also adopted in this paper.

From analysis above, the sleep posture recognition of human body includes skeleton keypoints estimation, angle of keypoints estimation and distance calculation of keypoints, etc. Based on them, the cross-validation is adopted, and then the final sleep postures are estimated.

2.3 | Quilt coverage area estimation

Let ρ denote the quilt coverage ratio of human body, and an estimation model was proposed in this paper to calculate the ρ. Based on it, the quilt coverage situation was obtained. Human skin color and quilt color

are different which can be recognized by the algorithm proposed. The estimation algorithm of quilt coverage area is shown as follows.

2.3.1 | Image preprocessing and optimal ROI

Image preprocessing plays an important role in the subsequent features extraction with deep network. The Gaussian filter processing was adopted in this paper, which is a linear smooth filtering, and the noise interference of image can be eliminated, including Gaussian noise, salt and pepper noise, etc. A user-specified template (convolution, mask, etc.) was used to scan each pixel in the image, and the weighted average gray value of the pixel in the template's neighborhood was used to replace the value of the pixel in the template's center.

In order to avoid the impact of bed objects other than the body and the quilt on the detection outcome, the corresponding area should be chosen for processing, that is, optimal region of interest (ROI) was extracted. The contour of the human body was extracted from the video by algorithm proposed and used as the optimal ROI area for subsequent processing.

2.3.2 | Quilt covered area

Binarization was applied to the optimized ROI region, and a specific gray scale binarization threshold value was chosen. Image binarization was the process of converting a grayscale image (with 256 different gray values ranging from 0 to 255) into a black-and-white image. Binarization processing was used to distinguish the quilt from human skin, as shown in Figure 3. Binarization processing should be completed separately for each color of the quilt.

Light colored quilt

If the quilt is light colored, the skin color appears darker than the quilt color in the surveillance image. In order to effectively distinguish the quilt from human skin, the gray value of the skin can be set to zero (black), and the gray value of the quilt can be set to 255 (white), which was shown in Equation (7). The coverage area of the quilt can be obtained by calculating the proportion of the white area in the ROI area. In this paper, Ω represents the coverage area of the quilt.

$$\Pi(x,y)=\begin{cases}0 & \text{skin}\\ 255 & \text{quilt}\end{cases} \tag{7}$$

where $\Pi(x,y)$ represents the gray value of this pixel.

Dark colored quilt

If the quilt is dark, the human skin color appears lighter than the quilt color in the video image. In order to distinguish human skin and quilt, the gray value of the image needs to be flipped firstly. Then,

FIGURE 3 An sleep image with binarization processing.

the gray value of the quilt and the skin was set, which was shown in Equation (8). Finally, the quilt coverage area Ω also can be calculated.

$$\Pi(x,y)=\begin{cases}0 & \text{quilt}\\ 255 & \text{skin}\end{cases} \tag{8}$$

As shown in Equation (9), the proportion of quilt coverage area Ω has been obtained, and the following quilt coverage conditions are defined by this value. The determination model of quilt coverage is defined as

$$\chi=\begin{cases}0 & \Omega\le c_1\\ 1 & c_1<\Omega\le c_2\\ 2 & c_2<\Omega\le c_3\\ 3 & c_3<\Omega\le c_4\\ 4 & c_4<\Omega\le c_5\end{cases} \tag{9}$$

where χ is the quilt coverage index, and $\chi=0$ represents no quilt, and $\chi=1$ means the quilt covers only the abdomen. $\chi=2$ means the quilt covers below the abdomen. $\chi=3$ denotes the quilt is covered below the neck, with arms outside the quilt. $\chi=4$ denotes the quilt is covered below the neck, with arms inside the quilt. Ω is the proportion of quilt covering, c_1, c_2, c_3, c_4, and c_5 represent the quilting partition values. Quilt cover partition values c_1, c_2, c_3, c_4, c_5 are given as follows: $c_1 \in [0.05, 0.15]$, $c_2 \in [0.25, 0.35]$, $c_3 \in [0.55, 0.65]$, $c_4 \in [0.7, 0.8]$, and $c_5 \in [0.85, 0.9]$. In this embodiment, $c_1=0.1$, $c_2=0.3$, $c_3=0.6$, $c_4=0.75$, $c_5=0.9$.

2.4 | Determination of thermal comfort

A determination model of human thermal comfort was established based on the body posture obtained in Section 2.2 and the quilt coverage obtained in Section 2.3 to determine the human thermal comfort. In particular, the sleeping positions and their accompanying thermal comfort status were examined using the human body posture and the quilt coverage area. In reality, the sleep postures used to assess thermal comfort are only a subset of all human postures. As a result, the thermal comfort-related posture types are fewer than the total number of human body postures. In this work, sleep postures are split into two categories: stretching postures and curling postures. The most striking quality of the stretching posture is that

the body is relaxed and the arms and legs are straight. Curled up postures are distinguished by the bent arms and legs. Based on this, the area covered by the quilt is calculated, including calculating whether the arm and legs are below or outside the quilt. There are a total of 10 sleeping postures, as illustrated in Table 1.

Therefore, the determination model of human thermal comfort is defined as follows:

$$\Upsilon = \begin{cases} 1 & (\psi = 0 \&\& \chi = 0) \| (\psi = 0 \&\& \chi = 3) \| (\psi = 0 \&\& \chi = 4) \ldots \| (\psi = 1 \&\& \chi = 2) \| (\psi = 1 \&\& \chi = 1); \\ 2 & (\psi = 0 \&\& \chi = 3) \| (\psi = 0 \&\& \chi = 1); \\ 3 & (\psi = 1 \&\& \psi = 0) \| (\psi = 1 \&\& \chi = 3) \| (\psi = 1 \&\& \chi = 4); \end{cases} \quad (10)$$

where Υ denotes the human comfort level. $\Upsilon = 1$ represents the body is in thermally comfort, $\Upsilon = 2$ represents the body is feeling hot, and $\Upsilon = 3$ represents the body is feeling cold. Further, $\psi = 0$ denotes the stretched sleep postures, and $\psi = 1$ represents the curling sleep postures. Essentially, forumla 13 is a confirmation of sleeping postures. The 10 sleeping postures shown in Table 1 and their corresponding thermal comfort levels were obtained from 438 questionnaires. Therefore, once the sleep posture detection is achieved through the various steps mentioned in 2.2 and 2.3, including Equation (10), the thermal comfort level is also determined.

In practice, the algorithm proposed in this paper can be embedded into hardware. Assume the hardware is called "the detection terminal of human thermal comfort," and the terminal incorporates the proposed algorithm, an infrared sensor, an RGB camera, an embedded motherboard, and so on. The real-time thermal comfort level of a sleeping person, as detected by the algorithm provided in this research, can be transformed to a control command that can regulate an air conditioner. As a result, better thermal comfort levels for the human body are possible. If the user feels cold, the terminal can send heating instructions to the air conditioner via an infrared transmitter. Cooling instructions can also be provided to the conditioner. If the user is at ease, the status quo will be preserved. It should be noted that the detecting terminal indicated above is not part of the major contribution scope of this research. The preceding explanation is intended to demonstrate how the algorithm suggested in this paper works in practical applications. Table 3 shows the major steps of the suggested algorithm.

TABLE 3 Algorithm flowchart (sleeping posture estimation of human thermal comfort).

Algorithm

Input: video during sleep;
Output: sleeping posture, human thermal comfort level
step:
1. Surveillance video preprocessing
  1. Frame extraction
  2. Denoising
  3. Obtain the best area (ROI)
2. Get keypoint coordinates
  1. Call the OpenPose platform
  2. Generate Jason file
3. Human body posture judgment
  1. Extract the coordinates of the point of interest from the Jason file
  2. Calculate the Euclidean distance between points
  3. Calculate the angle of the relevant included angle
  4. Define the threshold of leg bending as 160 degrees and the threshold of hand bending as 120 degrees. It is considered stretched if the leg angle or hand angle is more than the threshold. It is considered curled up if the leg or hand angle is less than the threshold.
  5. The threshold for both the leg and hand postures is set to 0.8. If the leg or hand distance is more than the threshold, the state is considered stretched. If the leg or hand distance is less than the threshold, it is determined to be curled up.
4. Estimation of quilt coverage area
  1. Gaussian filter denoising
  2. Choose the best area (ROI)
  3. Binarize the image with an appropriate threshold
  4. Calculate the area of light-colored quilt and dark quilt
5. Combine steps 3 and 4 to get the thermal comfort of the human body.

3 | RESULTS AND DISCUSSION

In order to validate the detection accuracy of the algorithm proposed, a total of 18 human subjects participated in a sleeping video recording test and 2.65 million frames of sleep posture were captured. First, the video data were processed, which included denoise, deblurring, and other effects. The algorithm training, validation, and optimization were then handled. This study was done on a 64-bit computer, and the technique was tested using 32 GB of memory. High-performance graphics processors are also required. As a result, the major validation server settings are as follows: (1) GPU: NVIDIA GeForce GTX 1080TI or 2080TI and (2) CPU: Intel(R) Xeon(R) CPU E5-2687 W v3@3.10GHz.

The 10 sleep postures are classified into three categories based on thermal comfort theory: warm sensation postures, comfortable sensation postures, and cold sensation postures. The proposed algorithm's detection accuracy is defined in Equation (11):

$$\Lambda_{\text{accuracy}} = \frac{F_{\text{correct}}}{F_{\text{total}}} \times 100\% \quad (11)$$

where F_{total} represents tthe sample space of each sleep posture, and F_{correct} is the posture images correctly detected in each sample space. The algorithm validation results reveal that the average accuracy of the algorithm suggested in this research is 91.15%. Figure 4 depicts the validation results of the suggested algorithm.

Thermal comfort is essential for both sleep quality and physical and mental wellness. However, there are currently no effective contactless technologies for detecting human thermal comfort when sleeping. This research proposes a method for detecting sleeping thermal comfort using a vision-based approach. Human thermal comfort changes throughout time, both between individuals and within individuals. The proposed algorithm is a method for real-time sensing. The method can handle frames at a rate of 24 or 30 frames per second. Individual disparities

can also be overcome by recording real-time posture fluctuation. The essential parameters were fine-tuned according to different postures during the algorithm design and debugging stages, and a comprehensive parameter was supplied in this work. Individual variations can thus be overcome by employing relevant and comprehensive factors.

The OpenPose was utilized to get the keypoint coordinates of the human body in order to determine the sleeping posture of the human body. It is worth noting that this approach is not exclusive to OpenPose. Other detection algorithms of human bone keypoints can also be chosen, and the sleeping posture of the human body can

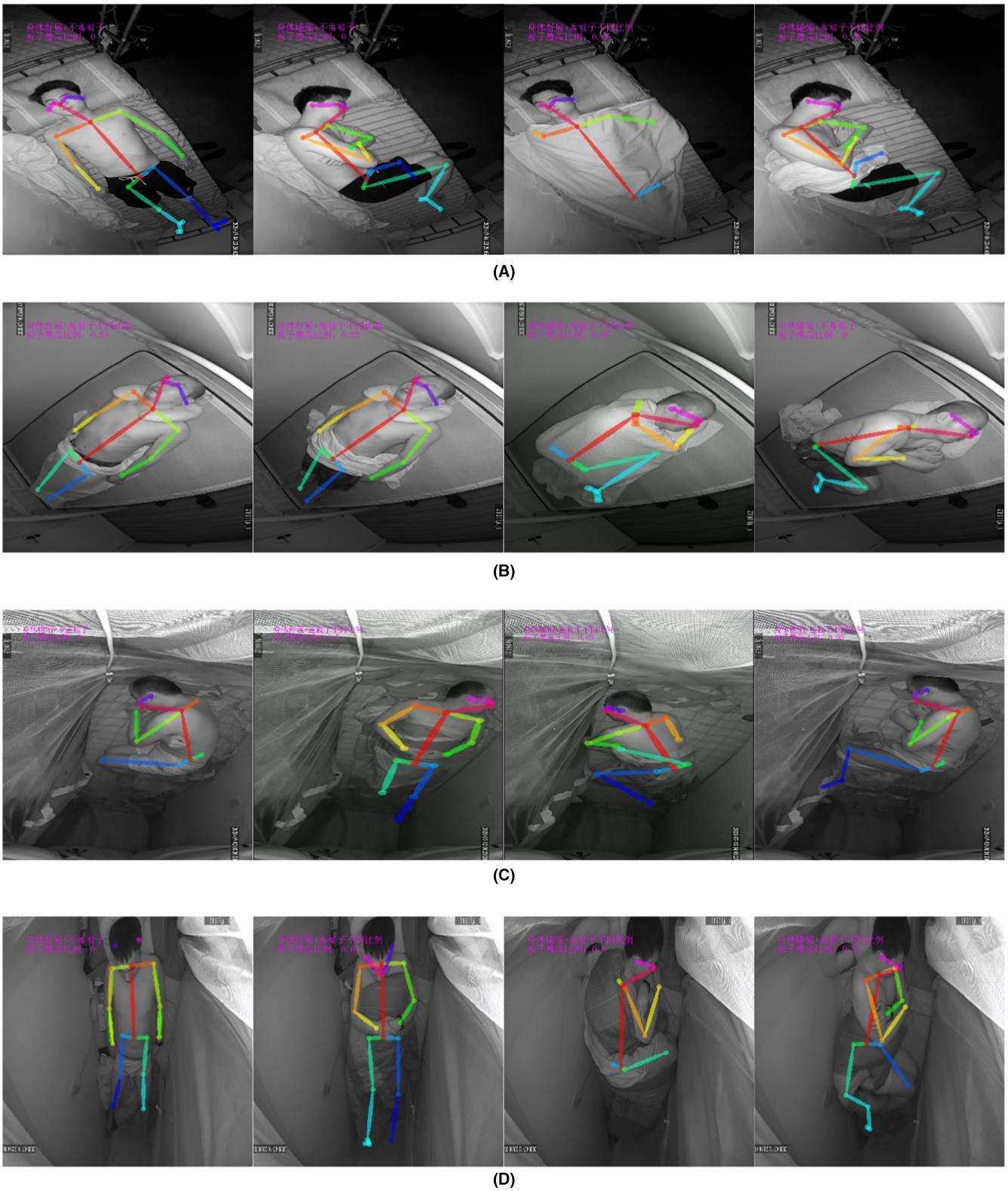

FIGURE 4 Algorithm validation results (A, B, C, and D denote different human subjects).

be derived utilizing the proposed algorithmic stages. The algorithm and a standard RGB camera can be installed and widely utilized in a computer server of an HVAC system in a building. The RGB camera's role is to capture data. In practice, to prevent infringing on user privacy, only the control signals generated by the suggested algorithm can be transferred without recording any user information.

Several frequent human postures and quilt covering conditions during sleep were defined in this research. The link between various sleeping postures, quilt covering conditions, and cold, warm, and comfortable thermal states were summarized using questionaries. Each person's sleeping posture is unique. The thermal comfort level of the eight postures depicted in Table 1 can be recognized by the respondents, according to the survey results. that is, respondents' assessments of the thermal comfort levels associated with these behaviors were relatively similar, and the fraction of respondents who held opposing views was modest. However, the other two postures, such as (1) body curled up, body part below neck covered with quilt, and arms covered beneath quilt and (2) body curled up, only belly of the body covered with quilt, while respondents were relatively consistent in their thermal comfort level for the sleep posture, the proportion was lower than that of the other eight postures. It demonstrates that individual variances in personal thermal comfort are evident.

During the algorithm validation, unexpected outcomes occurred on occasion. It usually happens in the early stages of recognizing sleeping postures or when the quilt covers a big section of the body. An detecting algorithm was built using the human skeletal keypoints. It comprises keypoint displacement, angle, and other parameters. The succeeding condition assessment will be incorrect if the skeleton keypoint was approximated inaccurately. The sleep posture will thus be inaccurately identified. Some optimized parameters were used in the method to avoid the aforementioned errors. Finally, typical image processing algorithms may have limits and inaccuracies when recognizing the region covered by the quilt. More deep learning methods will be built in the future to increase the performance of the suggested algorithm.

4 | FUTURE PERSPECTIVES

Based on our current knowledge, future research on human thermal comfort during sleep should concentrate on human health. The algorithm should be built or optimized in detail based on human health conditions. As a result, the physiological parameters of the human body can be detected efficiently to assess personal health status. This technology will be efficiently coupled with elder care in the future. More deep learning networks will be built in the future to improve algorithm detection performance.

5 | CONCLUSIONS

This study proposed a novel contactless detection approach of human thermal comfort during the sleeping state. In the first phase, 438 questions were answered, and 10 sleep postures of thermal comfort were defined. In the second phrase, a contactless detection algorithm was developed and validated. The conclusions are as follows.

1. Sleep thermal comfort can be assessed using sleeping posture recognition.
2. This paper's vision-based algorithm design is useful. Sleeping position can be estimated using the human skeleton keypoints. Furthermore, by combining sleeping position estimation with quilt coverage area calculation, thermal comfort may be estimated.
3. More sleeping aspects, such as sleeping posture and other information, can help to accurately estimate thermal comfort during the sleep stage.

More work will be required in the future to improve the algorithm's detection of more sleep postures. In practice, the algorithm proposed in this study can detect the thermal comfort level during sleep in real time and automatically adjust air conditioning parameters (set point temperature, supply air speed, on/off) to achieve energy efficient sleep thermal comfort while avoiding manual control in sleep state. Concerns about privacy can be resolved by ignoring identifying information, such as facial and body parts. Only the control command created by the suggested method was sent to the air conditioner.

AUTHOR CONTRIBUTIONS

XC and BY conceived and designed the study. FH, CX, and BY planned and conducted human tests. XC, BY, and FW wrote the initial manuscript draft. FW and TO involved in supervision, editing, and reviewing the manuscript. All authors involved in proofreading and editing of the final version of the manuscript.

ACKNOWLEDGMENTS

The project was financially supported by the Social Development Project of Jiangsu Key R&D Program (BE2022680), the National Natural Science Foundation of China (No. 52278119, No. 61972214), the Ministry of Industry and Information Technology of China (No. 2021-R-43), and Jiangsu Postdoctoral Science Foundation (1601039B). The authors appreciate Hui Zhang from University of California Berkeley for her suggestion.

CONFLICT OF INTEREST

The authors declare no conflict of interest. The funders had no contribution in this study, including the collection, analysis, interpretation of data, the writing of the manuscript, and the decision to publish the result.

DATA AVAILABILITY STATEMENT

The data that support the findings of this study are available on request from the corresponding author. The data are not publicly available due to privacy or ethical restrictions.

ORCID

Xiaogang Cheng https://orcid.org/0000-0002-5174-6422
Bin Yang https://orcid.org/0000-0003-4015-199X
Faming Wang https://orcid.org/0000-0002-2945-4685
Thomas Olofsson https://orcid.org/0000-0002-8704-8538

REFERENCES

1. Ding E. *Study on the Optimal Temperature, Air Velocity and Dynamic Change Patterns for Sleep Quality of Young People in the Hot-Humid Area of China*. Master Thesis. South China University of Technology; 2019.
2. U. S. Energy Information Administration (EIA). Annual Energy Outlook 2022, Washington, D. C.; 2022.
3. Stevner ABA, Vidaurre D, Cabral J, et al. Discovery of key whole-brain transitions and dynamics during human wakefulness and non-REM sleep. *Nat Commun*. 2019;10(1):1-14.
4. Energy market authority (EMA). Singapore Energy Statistics (SES 2021), Singapore; 2021.
5. Flemons WW. Obstructive sleep apnea. *N Engl J Med*. 2002;347(7):498-504.
6. Kemp B, Zwinderman AH, Tuk B, Kamphuisen HAC, Oberye JJL. Analysis of a sleep-dependent neuronal feedback loop: the slow-wave microcontinuity of the EEG. *IEEE Trans Biomed Eng*. 2000;47(9):1185-1194.
7. Cho SP, Lee J, Park HD, Lee KJ. Detection of arousals in patients with respiratory sleep disorders using a Single Channel EEG. *2005 IEEE Engineering in Medicine and Biology 27th Annual Conference*. IEEE; 2006:2733-2735.
8. Choi BH, Chung GS, Lee JS, Jeong DU, Park KS. Slow-wave sleep estimation on a load-cell-installed bed: a non-constrained method. *Physiol Meas*. 2009;30(11):1163-1170.
9. Tseng HW, Huang CD, Yen LY, Lin TW, Lee YW. A method of measuring sleep quality by using PPG. *2016 IEEE International Conference on Consumer Electronics-Taiwan (ICCE-TW)*. IEEE; 2016:1-2.
10. Kripke DF, Hahn EK, Grizas AP, et al. Wrist Actigraphic scoring for sleep laboratory patients: algorithm development. *J Sleep Res*. 2010;19(4):612-619.
11. Domingues A, Paiva T, Sanches JM. Sleep and wakefulness state detection in nocturnal actigraphy based on movement information. *IEEE Trans Biomed Eng*. 2013;61(2):426-434.
12. El-Manzalawy Y, Buxton O, Honavar V. Sleep/wake state prediction and sleep parameter estimation using unsupervised classification via clustering. *2017 IEEE International Conference on Bioinformatics and Biomedicine (BIBM 2017)*. IEEE; 2017:718-723.
13. Radha M, Fonseca P, Moreau A, et al. A deep transfer learning approach for wearable sleep stage classification with photoplethysmography. *NPJ Digital Med*. 2021;4(1):1-11.
14. Dafna E, Tarasiuk A, Zigel Y. Sleep-quality assessment from full night audio recordings of sleep apnea patients. *2012 Annual International Conference of the IEEE Engineering in Medicine and Biology Society*. IEEE; 2012:3660-3663.
15. Dafna E, Tarasiuk A, Zigel Y. Sleep-wake evaluation from whole-night non-contact audio recordings of breathing sounds. *PLoS One*. 2015;10(2):e0117382.
16. Wu H, Kato T, Numao M, Fukui KI. Statistical sleep pattern modelling for sleep quality assessment based on sound events. *Health Inf Sci Syst*. 2017;5(1):1-11.
17. Xue B, Deng B, Hong H, Wang Z, Zhu X, Feng DD. Non-contact sleep stage detection using canonical correlation analysis of respiratory sound. *IEEE J Biomed Health Inform*. 2019;24(2):614-625.
18. Peng YT, Lin CY, Sun MT, Landis CA. Multimodality sensor system for Long-term sleep quality monitoring. *IEEE Trans Biomed Circuits Syst*. 2007;1(3):217-227.
19. Choe J, Montserrat DM, Schwichtenberg AJ, Delp EJ. Sleep analysis using motion and head detection. *2018 IEEE Southwest Symposium on Image Analysis and Interpretation (SSIAI 2018)*. IEEE; 2018:29-32.
20. Cheng X, Yang B, Olofsson T, Liu G, Li H. A pilot study of online non-invasive measuring technology based on video magnification to determine skin temperature. *Build Environ*. 2017;121:1-10.
21. Cheng X, Yang B, Tan K, et al. A contactless measuring method of skin temperature based on the skin sensitivity index and deep learning. *Appl Sci*. 2019;9(7):1375.
22. Cheng X, Yang B, Hedman A, Olofsson T, Li H, van Gool L. NIDL: a pilot study of contactless measurement of skin temperature for intelligent building. *Energ Build*. 2019;198:340-352.
23. Meier A, Cheng X, Dyer W, Chris G, Olofsson T, Yang B. Non-invasive assessments of thermal discomfort in real time. *CATE 2019–Comfort at the Extremes: Energy, Economy and Climate*. Ecohouse Initative Ltd; 2019.
24. Yang B, Cheng X, Dai D, Olofsson T, Li H, Meier A. Real-time and contactless measurements of thermal discomfort based on human poses for energy efficient control of buildings. *Build Environ*. 2019;162:106284.
25. Qian J, Cheng X, Yang B, et al. Vision-based contactless pose estimation for human thermal discomfort. *Atmos*. 2020;11(4):376.
26. Li P, Dai P, Cao D, Liu B, Lu Y. Non-intrusive comfort sensing: detecting age and gender from infrared images for personal thermal comfort. *Build Environ*. 2022;219:109256.
27. Li P, Froese T, Brager G. Post-occupancy evaluation: state-of-the-art analysis and state-of-the-practice review. *Build Environ*. 2018;133:187-202.
28. X. Chen, A. L. Yuille. Articulated Pose Estimation By a graphical model with image dependent pairwise relations. Advances in neural information processing systems (NIPS 2014), Montreal, Quebec, Canada. Vol. 27; 2014.
29. Y. Chen, C. Shen, X. Wei, Liu L, Yang J. Adversarial Posenet: a structure-aware convolutional network for human pose estimation. Proceedings of the IEEE International Conference on Computer Vision (ICCV 2017), Venice, Italy; 2017:1212–1221.
30. A. Toshev, C. Szegedy. Deeppose: human pose estimation via deep neural networks. Proceedings of the IEEE Conference on Computer Vision and Pattern Recognition (CVPR 2014). Columbus, OH, USA; 2014:1653–1660.
31. T. Pfister, J. Charlies, A. Zisserman. Flowing Convnets for Human Pose Estimation in Videos. Proceedings of the IEEE International Conference on Computer Vision. Boston, MA, USA, 2015:1913–1921.
32. Y. Chen, Z. Wang, Y. Peng, Zhang Z, Yu G, Sun J. Cascaded pyramid network for multi-person pose estimation. Proceedings of the IEEE Conference on Computer Vision and Pattern Recognition (CVPR2018). Salt Lake City, Utah, USA; 2018:7103–7112.
33. L. Pishchulin, E. Insafutdinov, S. Tang, et al. Deepcut: joint subset partition and labeling for multi person pose estimation. Proceedings of the IEEE Conference on Computer Vision and Pattern Recognition (CVPR 2016). Las Vegas, Nevada, USA; 2016:4929–4937.
34. E. Insafutdinov, L. Pishchulin, B. Andres, Andriluka M, Schiele B. Deepercut: a deeper, stronger, and faster multi-person pose estimation model. European Conference on Computer Vision (ECCV2016). Amsterdam, Netherlands; 2016:34–50.
35. Cao Z, Hidalgo G, Simon T, Wei SE, Sheikh Y. OpenPose: realtime multi-person 2D pose estimation using part affinity fields. *IEEE Trans Pattern Anal Mach Intell*. 2019;43(1):172-186.
36. R. A. Güler, N. Neverova, I. Kokkinos. Densepose: dense human pose estimation in the wild. Proceedings of the IEEE Conference on Computer Vision and Pattern Recognition (CVPR 2018). Salt Lake City, Utah, USA; 2018:7297–7306.

37. J. Li, C. Wang, H. Zhu, Mao Y, Fang HS, Lu C. Crowdpose: efficient crowded scenes pose estimation and a new benchmark. Proceedings of the IEEE/CVF Conference on Computer Vision and Pattern Recognition (CVPR 2019). Long Beach, CA, USA; 2019:10863–10872.
38. G. Christie, R. R. R. M. Abujder, K. Foster, Hagstrom S, Hager GD, Brown MZ. Learning geocentric object pose in oblique monocular images. Proceedings of the IEEE/CVF conference on computer vision and pattern recognition (CVPR 2020). Virtual; 2020:14512–14520.
39. J. Wang, C. Wen, Y. Fu, et al. Neural pose transfer by spatially adaptive instance normalization. Proceedings of the IEEE/CVF conference on computer vision and pattern recognition (CVPR 2020). Virtual; 2020:5831–5839.
40. B. Artacho, A. Savakis. Unipose: unified human pose estimation in single images and videos. Proceedings of the IEEE/CVF conference on computer vision and pattern recognition. Virtual; 2020:7035–7044.
41. K. Li, S. Wang, X. Zhang, Xu Y, Xu W, Tu Z. Pose recognition with Cascade transformers. Proceedings of the IEEE/CVF conference on computer vision and pattern recognition (CVPR 2021). Virtual; 2021:1944–1953.
42. Z. Geng, K. Sun, B. Xiao, Zhang Z, Wang J. Bottom-up human pose estimation via disentangled Keypoint regression. Proceedings of the IEEE/CVF conference on computer vision and pattern recognition (CVPR 2021). Virtual; 2021:14676–14686.
43. L. Schmidtke, A. Vlontzos, S. Ellershaw, Lukens A, Arichi T, Kainz B Unsupervised human pose estimation through transforming shape templates. Proceedings of the IEEE/CVF conference on computer vision and pattern recognition (CVPR 2021). Virtual; 2021:2484–2494.
44. C. M. Parameshwara, G. Hari, C. Fermüller, Sanket NJ, Aloimonos Y. DiffPoseNet: direct differentiable camera pose estimation. Proceedings of the IEEE/CVF Conference on Computer Vision and Pattern Recognition (CVPR 2022). New Orleans, Louisiana, USA; 2022:6845–6854.
45. K. Bartol, D. Bojanić, T. Petković, Pribanić T. Generalizable human pose triangulation. Proceedings of the IEEE/CVF Conference on Computer Vision and Pattern Recognition (CVPR 2022). New Orleans, Louisiana, USA; 2022:11028–11037.
46. I. Shugurov, F. Li, B. Busam, Ilic S. OSOP: a multi-stage one shot object pose estimation framework. Proceedings of the IEEE/CVF Conference on Computer Vision and Pattern Recognition (CVPR 2022). New Orleans, Louisiana, USA; 2022:6835–6844.
47. Mohammadi SM, Enshaeifar S, Hilton A, Dijk DJ, Wells K. Transfer learning for clinical sleep pose detection using a single 2D IR camera. *IEEE Trans Neural Syst Rehabil Eng*. 2020;29:290-299.
48. Piriyajitakonkij M, Warin P, Lakhan P, et al. SleepPoseNet: multi-view learning for sleep postural transition recognition using UWB. *IEEE J Biomed Health Inform*. 2020;25(4):1305-1314.

How to cite this article: Cheng X, Hu F, Yang B, Wang F, Olofsson T. Contactless sleep posture measurements for demand-controlled sleep thermal comfort: A pilot study. *Indoor Air*. 2022;32:e13175. doi:10.1111/ina.13175